Realization of the Einstein-Podolsky-Rosen Paradox for Continuous Variables

Z. Y. Ou, S. F. Pereira, H. J. Kimble, and K. C. Peng[(a)]
Norman Bridge Laboratory of Physics 12-33, California Institute of Technology, Pasadena, California 91125
(Received 20 February 1992)

The Einstein-Podolsky-Rosen paradox is demonstrated experimentally for dynamical variables having a continuous spectrum. As opposed to previous work with discrete spin or polarization variables, the continuous optical amplitudes of a signal beam are inferred in turn from those of a spatially separated but strongly correlated idler beam generated by nondegenerate parametric amplification. The uncertainty product for the variances of these inferences is observed to be 0.70 ± 0.01, which is below the limit of unity required for the demonstration of the paradox.

PACS numbers: 03.65.Bz, 42.50.Wm

Over the past twenty years, a variety of experiments have investigated the violations by quantum mechanics of the constraints imposed by local realism as codified by the Bell inequalities [1,2]. Of particular importance have been optical experiments which are based upon observations of correlations for spatially separated photon pairs generated either in an atomic cascade [2,3] or by parametric down-conversion [4]. However, without exception, these measurements as well as those in other systems [2] have followed Bohm's suggestion [5] and have involved discrete (dichotomic) variables for which the Bell inequalities are applicable. By contrast, an experiment to demonstrate the original proposal by Einstein, Podolsky, and Rosen (EPR) [6] for a system of observables with a continuous spectrum has not been previously realized. Indeed, although there are theoretical examples [7,8] of the violation of locality inequalities [2], there unfortunately exists no general formalism for describing measurements of correlations of continuous variables which *a priori* provides sufficient conditions for the elimination of the whole class of local realistic theories.

With reference to the original gedanken experiment of EPR [6], the question of the irreducible nonlocality of quantum mechanics [1] can be addressed by way of the Wigner phase-space distribution [9] since the relevant dynamical variables are the positions and momenta for two correlated particles. As shown by Bell [7] and others [8,10], the Wigner function in this case is everywhere non-negative and hence provides a local, realistic description of the correlations discussed by EPR. Hence ironically, the correlations of EPR [6] are not manifestly quantum but rather are "precisely those between two classical particles in independent free classical motion [7]." Nonetheless, the issue of the generalization of the Bell inequalities [1,2] to dynamical variables with continuous spectra remains an important challenge.

Motivated both by the historical significance of the EPR paradox and as well by the epistemological issue outlined above, we present in this Letter an experimental realization of the EPR paradox for continuous variables [6]. Our work follows the avenue suggested by Reid and Drummond [11,12] and employs a subthreshold nondegenerate optical parametric oscillator to generate correlated amplitudes for signal and idler beams of light. In the limiting case of infinite parametric gain, the wave function of an ideal system of this type is of the same form as the one originally discussed by EPR [6]. The roles of canonical position and momentum variables in the EPR script are played by the quadrature-phase amplitudes of the signal and idler beams, where the amplitudes of the signal beam (X_s, Y_s) are inferred in turn from measurements of the spatially separated amplitudes (X_i, Y_i) of the idler beam. The errors of these inferences are quantified by the variances $\Delta^2_{\rm inf}X$ and $\Delta^2_{\rm inf}Y$, with the EPR paradox requiring that $\Delta^2_{\rm inf}X\,\Delta^2_{\rm inf}Y < 1$ [6,11,12]. In our measurements we have observed $\Delta^2_{\rm inf}X\,\Delta^2_{\rm inf}Y = 0.70 \pm 0.01$, thus demonstrating the paradox.

Our experiment is depicted in simple conceptual terms in Fig. 1(a), where two initially independent fields interact by way of nondegenerate parametric amplification

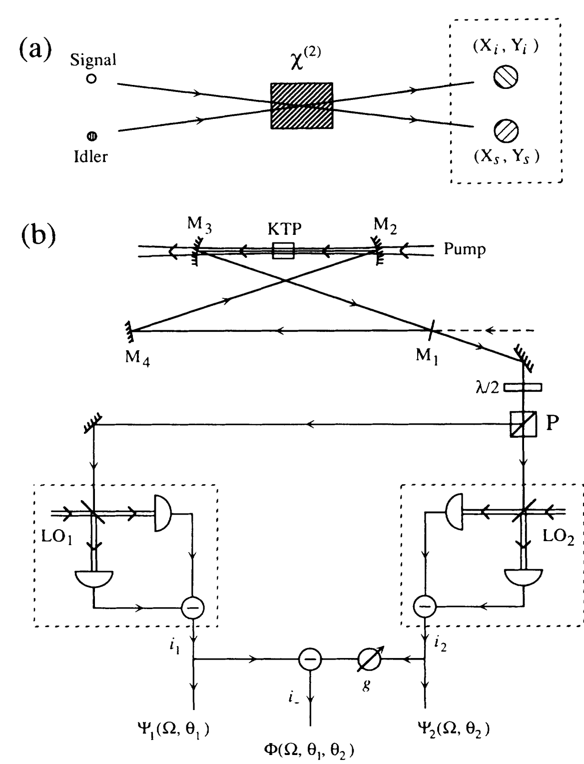

FIG. 1. (a) Scheme for realization of the EPR paradox by nondegenerate parametric amplification, with the optical amplitudes (X_s, Y_s) inferred in turn from (X_i, Y_i). (b) Principal components of the experiment.

and then separate. Given that the two outgoing beams are strongly correlated ($X_i \to X_s$ and $-Y_i \to Y_s$ in the ideal case), our objective is to make measurements of $(X_i, -Y_i)$ for the output quadrature-phase amplitudes of the idler beam in order to infer (at a distance) the corresponding values of (X_s, Y_s) for the signal beam. Since the measurements are not perfect nor is the degree of correlation between the two beams 100%, we employ the scaled amplitudes $(g_x X_i, -g_y Y_i)$ as our estimators of (X_s, Y_s) [11,12]. The errors of the interferences are then quantified by the variances $\Delta^2_{\rm inf}X \equiv \langle (\tilde{X}_s - g_x \tilde{X}_i)^2 \rangle$ and $\Delta^2_{\rm inf}Y \equiv \langle (\tilde{Y}_s + g_y \tilde{Y}_i)^2 \rangle$ with $\tilde{A} \equiv A - \langle A \rangle$, where the quantities $g_{x,y}$ $(0 \le g_{x,y} \le 1)$ are chosen to minimize the variances and hence to optimize our inference based upon the less than ideal degree of correlation. The normalization is such that $\Delta^2_{\rm inf}X < 1$ implies that X_s for the signal beam can be determined from measurements of X_i for the idler beam to better than the vacuum-state limit for the signal beam alone (and likewise for $\Delta^2_{\rm inf}Y$). A measurement of $g_x X_i$ thus specifies X_s to an error $\Delta_{\rm inf}X$, while a measurement of $-g_y Y_i$ specifies Y_s to an error $\Delta_{\rm inf}Y$. Following the discussion of EPR, we then assign objective values to (X_s, Y_s) to within the errors $(\Delta_{\rm inf}X, \Delta_{\rm inf}Y)$, with a paradox arising for $\Delta^2_{\rm inf}X \Delta^2_{\rm inf}Y < 1$ since quantum mechanics demands that $\Delta^2 X_s \Delta^2 Y_s \ge 1$, where $\Delta^2 A \equiv \langle \tilde{A}^2 \rangle$. Of course the apparent contradiction between these inequalities is not fundamental and is resolved in the quantum theory by noting that the conditional distribution for X_s given X_i (from which $\Delta^2_{\rm inf}X$ follows) does not coincide with the unconditional distribution for X_s itself (from which $\Delta^2 X_s$ follows) and similarly for $Y_{s,i}$.

As for the practical implementation of this general discussion, we turn to a more detailed discussion of our actual experiment as illustrated in Fig. 1(b). Frequency degenerate but orthogonally polarized signal and idler fields are generated by type-II down-conversion in a subthreshold optical parametric oscillator (OPO) formed by a folded ring cavity containing a crystal of potassium titanyl phosphate (KTP). Relative to our earlier work [13], a significant technical advance is the use of *a*-cut KTP at 1.08 μm to achieve *noncritical* phase matching [14,15] thus minimizing problems with beam walkoff and polarization mixing. The KTP crystal is of length 10 mm, is antireflection coated for 1.08 and 0.54 μm, and has a measured single-pass harmonic conversion efficiency of 6×10^{-4}/W for our geometry. The total intracavity passive losses at 1.08 μm are 0.32% and the transmission coefficient of the output mirror M_1 is 3%. The OPO is pumped by green light at 0.54 μm generated by intracavity frequency doubling in a frequency-stabilized Nd:YAP laser, with the OPO cavity locked to the laser frequency with a weak countercirculating injected beam. Simultaneous resonance for the signal and idler fields is achieved by adjusting the temperature of the KTP crystal with mK precision. The pump field at 0.54 μm is itself resonant in a separate and independently locked buildup cavity (enhancement $\sim 5\times$).

The quadrature-phase amplitudes of the fields emerging from the OPO are detected by two separate balanced homodyne receivers with homodyne efficiencies $(\eta_1, \eta_2) = (0.95, 0.96)$ and quantum efficiencies $(\alpha_1, \alpha_2) = (0.90, 0.80)$ (Fig. 1) [16,17]. As a prelude to measurements of EPR correlations, we first examine squeezed-state generation by the system, which for a type-II process results from the projection of signal and idler modes along polarization directions at $\pm 45°$ to these modes [18]. A half-wave plate ($\lambda/2$) and a polarizer (P) at the output of the OPO serve to direct either the signal and idler beams or the $\pm 45°$ projections to the two sets of balanced detectors. In Fig. 2 we present results from measurements of the spectral density $\Psi_1(\Omega, \theta_1)$ for the fluctuations of the photocurrent i_1 for a single squeezed beam. Here Ω is the (fixed) rf analysis frequency, and θ_1 is the phase offset between the local oscillator LO_1 and the squeezed input which is scanned to achieve maximum (minimum) noise level denoted by Ψ_+ (Ψ_-). The noise level Ψ_0 for a vacuum-state input is determined to within ± 0.1 dB [17], while the quantum noise gain G_q for the OPO is calculated from the squeezing trace itself $[G_q = (\Psi_+ + \Psi_-)/2\Psi_0]$. The two full curves are theoretical results for $\Psi_\pm$ [11,19], with the overall detection efficiency for best fit found to be $\xi = 0.63$. This value compares favorably with the overall efficiency of 0.69 derived from measurements of the individual losses (cavity escape efficiency $\rho = 0.90$ and propagation efficiency $\zeta = 0.95$, together with η_1, α_1). Note that the data in Fig. 2 are directly from observation without adjustment (in particular, the thermal noise level of the detectors lies 25 dB below Ψ_0). For green pump power of 80 mW, the largest degree of observed nonclassical noise reduction is -3.6 ± 0.2 dB relative to the vacuum-state limit for a single squeezed beam.

Although the fields formed from the superposition of signal and idler beams are squeezed, the signal and idler beams taken individually show no such nonclassical behavior. In fact either beam on its own should have statis-

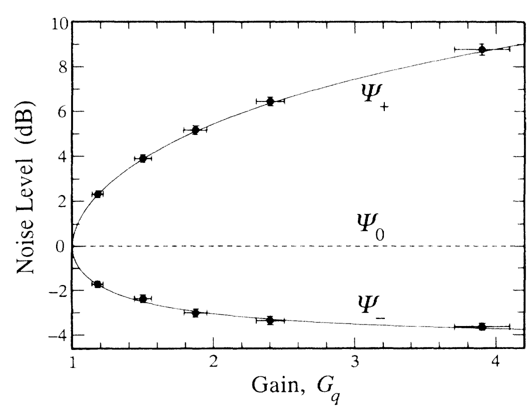

FIG. 2. Logarithm of observed noise levels Ψ_+ (maximum) and Ψ_- (minimum) vs OPO gain G_q for a squeezed beam at balanced detector 1 (cf. Fig. 1). Ψ_0 is the vacuum-state level and $\Omega/2\pi = 1.1$ MHz for these data. The solid curves are theoretical fits as discussed in the text.

tics indistinguishable from narrow-band thermal light [20]. On the other hand, these excess fluctuations are strongly correlated (as documented in Fig. 2) such that for large gain in a lossless system, the quadrature amplitudes of the signal and idler beams become "quantum copies" of one another over a bandwidth set by the OPO linewidth. We investigate this correlation experimentally by way of the difference photocurrent $i_- = i_1 - g i_2$, where the balanced detector 1 is illuminated with the signal field and balanced detector 2 with the idler field. From the spectral density of photocurrent fluctuations $\Phi(\Omega,\theta_1,\theta_2)$ for i_- we can determine the quantities $(\Delta^2_{\rm inf}X(\Omega), \Delta^2_{\rm inf}Y(\Omega))$, where now we are dealing with the spectral components $(X_{s,i}(\Omega), Y_{s,i}(\Omega))$ of the quadrature-phase amplitudes. Although some attention must be given to the issue that $(X_{s,i}(\Omega), Y_{s,i}(\Omega))$ are not Hermitian, the EPR paradox can nonetheless be phrased in terms of the measured spectral noise levels as the simple requirement that $\Delta^2_{\rm inf}X(\Omega)\Delta^2_{\rm inf}Y(\Omega) < 1$ [12,19].

Results from our measurements of $\Phi(\Omega,\theta_1,\theta_2)$ are displayed in Fig. 3, where the noise levels associated with $\Delta^2_{\rm inf}X(\Omega)$ and $\Delta^2_{\rm inf}Y(\Omega)$ are shown sequentially by stepping the phases (θ_1,θ_2) between the local oscillator beams $(\mathrm{LO}_1,\mathrm{LO}_2)$ and the signal and idler fields with piezoelectrically mounted mirrors. Denoting the general quadrature amplitudes of the signal and idler fields by

$$Z_{s,i}(\Omega,\phi_{s,i}) \equiv \int d\Omega\, [a_{s,i}(\Omega)e^{-i\phi_{s,i}} + a^\dagger_{s,i}(-\Omega)e^{i\phi_{s,i}}]$$

with a ($a^\dagger$) as the annihilation (creation) operator for the field at offset Ω from the optical carrier and with the integration over a small interval $\Delta\Omega$ around Ω, we have

$$\Phi(\Omega,\theta_1,\theta_2)\Delta\Omega \sim \langle |\tilde{Z}_s(\Omega,\theta_1) - g\tilde{Z}_i(\Omega,\theta_2)|^2 \rangle$$

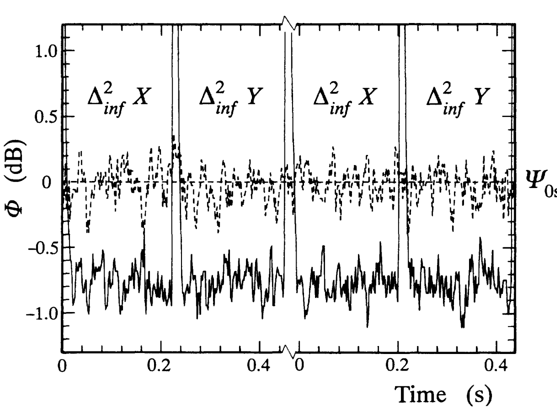

FIG. 3. Spectral density of photocurrent fluctuations $\Phi(\Omega,\theta_1,\theta_2)$ vs time with the vacuum-noise level for the signal beam alone given by Ψ_{0s}. The phases (θ_1,θ_2) are chosen first to record the variance $\Delta^2_{\rm inf}X(\Omega)$ and are then stepped to record $\Delta^2_{\rm inf}Y(\Omega)$. Two separate measurements of $(\Delta^2_{\rm inf}X(\Omega), \Delta^2_{\rm inf}Y(\Omega))$ are shown. The large increases in Φ arise in passing through a noise maximum as $\theta_1+\theta_2 \rightarrow \theta_1+\theta_2+2\pi$. Acquisition parameters $\Omega/2\pi = 1.1$ MHz, rf bandwidth $\Delta\Omega/2\pi = 100$ kHz, video bandwidth $= 0.2$ kHz, and $g^2 = 0.58$ for minimum noise.

(Ref. [21]). Since for a nondegenerate parametric amplifier Φ depends only upon $\theta_1+\theta_2$, we vary a common overall phase θ_0 (where $\theta_{1,2} = \theta_0 + \delta\theta_{1,2}$) until Φ is minimized. The quadrature phases that are then measured at the two balanced detectors are denoted by $Z_s(\theta_1) \equiv X_s$ and $Z_i(\theta_2) \equiv X_i$, with now $\Phi \sim \langle |(\tilde{X}_s - g\tilde{X}_i)|^2 \rangle / \Delta\Omega \equiv \Delta^2_{\rm inf}X(\Omega)$. The phases are next incremented with $\theta_0 \rightarrow \theta_0 + \pi/2$, $\delta\theta_1 \rightarrow \delta\theta_1 + \pi$, and $\delta\theta_2 \rightarrow \delta\theta_2$, such that $Z_s(\theta_1) \rightarrow Z_s(\theta_1 + 3\pi/2) \equiv -Y_s$ and $Z_i(\theta_2) \rightarrow Z_i(\theta_2 + \pi/2) \equiv Y_i$, with now $\Phi \sim \langle |(\tilde{Y}_s + g\tilde{Y}_i)|^2 \rangle / \Delta\Omega \equiv \Delta^2_{\rm inf}Y(\Omega)$. The phase steps are calibrated independently with an interferometer to within about 4°. For example, in Figs. 3 and 4, θ_0 is stepped by $94° \pm 1°$, while θ_1 is stepped by $180° \pm 4°$. We thus record the variance $\Delta^2_{\rm inf}X(\Omega)$ associated with one pair of quadrature amplitudes (X_s, X_i) followed by the variance $\Delta^2_{\rm inf}Y(\Omega)$ associated with the (approximately) conjugate pair (Y_s, Y_i). These variances then specify the error in our inference of (X_s, Y_s) from measurements (at a distance) of $(g_x X_i, -g_y Y_i)$.

From Fig. 3 it is clear that both $\Delta^2_{\rm inf}X(\Omega)$ and $\Delta^2_{\rm inf}Y(\Omega)$ lie below the level of unity associated with the vacuum-state fluctuations of the signal beam alone ($g^2 = 0$). Indeed for this trace we have that $\Delta^2_{\rm inf}X(\Omega) = 0.835 \pm 0.008$ and $\Delta^2_{\rm inf}Y(\Omega) = 0.837 \pm 0.008$ with $g_x^2 = g_y^2 \equiv g^2 = 0.58$, so that $\Delta^2_{\rm inf}X(\Omega)\Delta^2_{\rm inf}Y(\Omega) = 0.70 \pm 0.01 < 1$, thus providing an experimental realization of the EPR paradox. We should emphasize that although $\Delta^2_{\rm inf}X(\Omega) < 1$ is the relevant criterion for the EPR paradox, the observation $\Delta^2_{\rm inf}X(\Omega) < 1 + g^2$ itself violates a classical Cauchy-Schwartz inequality and hence is associated with a nonclassical field [12]. For the data in Fig. 3, we find that $10\log[\Delta^2_{\rm inf}X(\Omega)/(1+g^2)] \simeq -2.8$ dB. On the other hand, the noise levels $\Psi_{1,2}$ for signal and idler beams taken individually [from photocurrents (i_1, i_2)] are observed to be phase insensitive and to lie 4.1 dB (2.6×) above their respective vacuum-state limits.

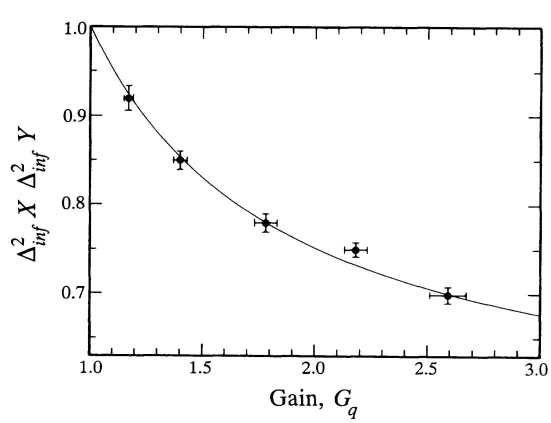

FIG. 4. Product of inference variances $\Delta^2_{\rm inf}X(\Omega)\Delta^2_{\rm inf}Y(\Omega)$ vs interaction strength G_q. The level unity is associated with the vacuum-state limit for the signal beam alone. Demonstration of the EPR paradox requires $\Delta^2_{\rm inf}X(\Omega)\Delta^2_{\rm inf}Y(\Omega) < 1$. The solid theoretical curve is as discussed in the text.

In Fig. 4 we collect results for the product $\Delta^2_{\rm inf}X(\Omega)\times\Delta^2_{\rm inf}Y(\Omega)$ obtained from measurements as in Fig. 3 for five different values of quantum noise gain G_q, which is determined from the level of phase-insensitive noise for the signal beam alone ($G_q=\Psi_1/\Psi_{0_s}$). Also shown in Fig. 4 is the theoretical result that we have calculated along the lines of the work in Refs. [11,12], but generalized to include the losses in the experiment [19]. With the detection efficiencies determined as in Fig. 2, there are otherwise no adjustable parameters in the comparison of theory and experiment. Note that the error bars in Fig. 4 are meant to indicate the uncertainties in G_q and $\Delta^2_{\rm inf}X\Delta^2_{\rm inf}Y$ associated with trace-to-trace drifts in the green pump power and in the vacuum-state level; the statistical uncertainty of $\Delta^2_{\rm inf}X\Delta^2_{\rm inf}Y$ from a single trace is much smaller than shown by the vertical error bars. Within these uncertainties, there is evidently reasonable quantitative agreement between theory and experiment.

In summary, we have presented an experimental realization of the EPR paradox [6] for continuous variables. Although our detectors for the signal and idler beams are not causally separated, there seems to be little motivation to achieve a spacelike separation since the issue of local realism is made irrelevant by the fact that the Wigner phase-space function provides a local realistic (hidden variable) description for our experiment as well as for the original EPR gedanken experiment. On the other hand, there remains the challenge of extending these initial measurements to situations of nonequivalence for quantum mechanics and local realism with respect to variables with a continuous spectrum. For example, if the vacuum-state inputs to our system were replaced with a single-photon state, the Wigner distribution for the output fields would be negative in some region and hence would no longer serve as the basis for a local hidden-variable theory. While this would certainly seem to be a necessary condition for a locality violation [7], the possible existence of an alternative phase-space distribution (from the infinite class of possibilities) which provides a local realistic description is not excluded *a priori* since there is no generalization of the Bell inequalities [1,2] for continuous variables. Apart from this fundamental issue, our experiment should also have application to precision measurement since the correlations evidenced in Figs. 4 and 5 can be employed for noise suppression below the vacuum-state limit in various dual-beam arrangements. It is also of interest to explore applications to quantum communication, since information encoded on the signal beam with small signal-to-noise ratio can nonetheless be extracted with high signal-to-noise ratio by way of the quantum copy provided by the idler beam [22].

We gratefully acknowledge the contributions of S. Braunstein, C. M. Caves, P. D. Drummond, J. L. Hall, and M. D. Reid. This work was supported by the Office of Naval Research, by the National Science Foundation, and by the Venture Research Unit of BP.

[a]Permanent address: Shanxi University, Taiyuan, Shanxi, People's Republic of China 030006.

[1] J. S. Bell, *Speakable and Unspeakable in Quantum Mechanics* (Cambridge Univ. Press, Cambridge, 1988).

[2] J. F. Clauser and A. Shimony, Rep. Prog. Phys. **41**, 1881 (1978), and references therein.

[3] A. Aspect, J. Dalibard, and G. Roger, Phys. Rev. Lett. **49**, 1804 (1982); W. Pierre *et al.*, *ibid.* **54**, 1790 (1985).

[4] Y. H. Shih and C. O. Alley, Phys. Rev. Lett. **61**, 2921 (1988); Z. Y. Ou and L. Mandel, *ibid.* **61**, 50 (1988); J. G. Rarity and P. R. Tapster, *ibid.* **64**, 2495 (1990).

[5] D. Bohm, *Quantum Theory* (Prentice-Hall, Englewood Cliffs, NJ, 1951).

[6] A. Einstein, B. Podolsky, and N. Rosen, Phys. Rev. **47**, 777 (1935).

[7] Bell, (Ref. [1]), p. 196.

[8] A. M. Cetto, L. De La Pena, and E. Santos, Phys. Lett. **113A**, 304 (1985).

[9] E. P. Wigner, Phys. Rev. **40**, 749 (1932).

[10] S. L. Braunstein and C. M. Caves (private communication).

[11] M. D. Reid and P. D. Drummond, Phys. Rev. Lett. **60**, 2731 (1988); Phys. Rev. A **41**, 3930 (1990).

[12] M. D. Reid, Phys. Rev. A **40**, 913 (1989).

[13] S. F. Pereira, K. C. Peng, and H. J. Kimble, in *Coherence and Quantum Optics IV*, edited by J. H. Eberly, L. Mandel, and E. Wolf (Plenum, New York, 1990), p. 889.

[14] V. M. Garmash *et al.*, Pis'ma Zh. Tekh. Fiz. **12**, 1222 (1986) [Sov. Tech. Phys. Lett. **12**, 505 (1986)].

[15] Z. Y. Ou *et al.*, Opt. Lett. **17**, 640 (1992).

[16] H. P. Yuen and V. W. S. Chan, Opt. Lett. **8**, 177 (1983).

[17] L. A. Wu, M. Xiao, and H. J. Kimble, J. Opt. Soc. Am. B **4**, 1465 (1987).

[18] P. Grangier *et al.*, Phys. Rev. Lett. **59**, 2153 (1987).

[19] Z. Y. Ou, S. F. Pereira, and H. J. Kimble (to be published).

[20] S. M. Barnett and P. L. Knight, J. Opt. Soc. Am. B **2**, 467 (1985).

[21] Note that $\Delta^2_{\rm inf}X(\Omega)$, $\Delta^2_{\rm inf}Y(\Omega)$, and $\Phi(\Omega)$ can be expressed in terms of the Hermitian operators Re[$Z_{s,i}$] and Im[$Z_{s,i}$] as discussed in Refs. [12,19].

[22] C. K. Hong, S. R. Friberg, and L. Mandel, Appl. Opt. **24**, 3877 (1985).